ELSEVIER

Biochemical Pharmacology 64 (2002) 1689–1701

Biochemical Pharmacology

Mobilization of intracellular iron by analogs of pyridoxal isonicotinoyl hydrazone (PIH) is determined by the membrane permeability of the iron–chelator complexes

Joan L. Buss, Emmanuele Arduini, Prem Ponka*

Departments of Physiology and Medicine, McGill University and Lady Davis Institute for Medical Research, Sir Mortimer B. Davis Jewish General Hospital, 3755 Chemin de la Cote-Ste-Catherine, Montreal, Que., Canada H3T 1E2

Received 6 March 2002; accepted 8 May 2002

Abstract

In the ongoing search for an effective, orally active iron–chelator, the capacity of a series of halogenated analogs of pyridoxal isonicotinoyl hydrazone (PIH) to bind intracellular ^{59}Fe and cause its release from cells was investigated. Reticulocytes labeled with $^{59}Fe_2$-transferrin in which heme synthesis was inhibited by succinylacetone were used as a model of ^{59}Fe mobilization. The kinetics of iron binding were similar for all the chelators tested (half-time of approximately 1 hr), and all bound more than twice as much ^{59}Fe as PIH. The rate of release of the ^{59}Fe–chelator complexes from cells depended upon the structure of the chelators. *Ortho*-substituted analogs were more effective at mobilizing cellular iron than *meta* and *para* isomers, due to a more efficient release of the iron complexes from the cell. The iron–chelator complexes which were released slowly from cells had a high affinity for erythrocyte ghost membranes, indicating the role of membrane permeability in the release mechanism of the complexes. The addition of BSA to the extracellular medium increased the extent of iron release by lipophilic analogs in a concentration-dependent manner, presumably by acting as a sink for the lipophilic complexes. The affinity of BSA for the chelators and their Fe^{3+} complexes, determined spectrophotometrically, demonstrated that all chelators and their iron complexes bound BSA with dissociation constants ranging from 7,000 to >500,000 M^{-1}. Understanding the importance of the rate of release of the iron–chelator complex will direct the search for iron–chelators with improved efficacy.

Keywords: Iron–chelators; Pyridoxal isonicotinoyl hydrazone (PIH); PIH analogs; Membrane permeability of iron chelates; Mobilization of iron from cells; Secondary iron overload

1. Introduction

Iron has many uses in biological systems because of its unsurpassed catalytic versatility. However, the chemical properties of iron that allow this versatility are also responsible for its potential toxicity. Iron in excess, due to its catalysis of one-electron redox chemistry, plays a key role in the formation of oxygen radicals, which cause oxidative damage to cellular structures [1]. Iron metabolism in humans is characterized by limited external exchange, and efficient re-utilization from internal sources. Because of the limited ability of the body to excrete excess iron, iron overload develops in transfusion-dependent patients, such as those with β-thalassemia, aplastic anemia, or myelodysplastic syndrome. The only treatment for secondary iron overload is the administration of iron chelating agents [2,3].

Desferrioxamine is the only iron–chelator in routine clinical use, but this drug is not absorbed orally and has a very short plasma half-time [4]. Hence, desferrioxamine treatment involves subcutaneous infusion for up to 12 hr a day, and patient noncompliance is high. Although the orally active chelator 1,2-dimethyl-3-hydroxypyrid-4-one (deferiprone, L1) increases urinary iron excretion, there are many serious complications associated with deferiprone therapy, including agranulocytosis and arthritis [2,3].

New orally effective iron–chelators are urgently needed, and PIH (structure shown in Fig. 1), whose capacity to mobilize iron has been recognized *in vitro* [5] and *in vivo* [6], shows promise for the treatment of secondary iron

* Corresponding author. Tel.: +1-514-340-8222 ext. 5289; fax: +1-514-340-7502.

E-mail address: prem.ponka@mcgill.ca (P. Ponka).

Abbreviations: FBS, fetal bovine serum; MEM, minimal essential medium; PBH, pyridoxal benzoyl hydrazone; PIH, pyridoxal isonicotinoyl hydrazone; and SIH, salicylaldehyde isonicotinoyl hydrazone.

0006-2952/02/$ – see front matter © 2002 Published by Elsevier Science Inc.
PII: S0006-2952(02)01426-0

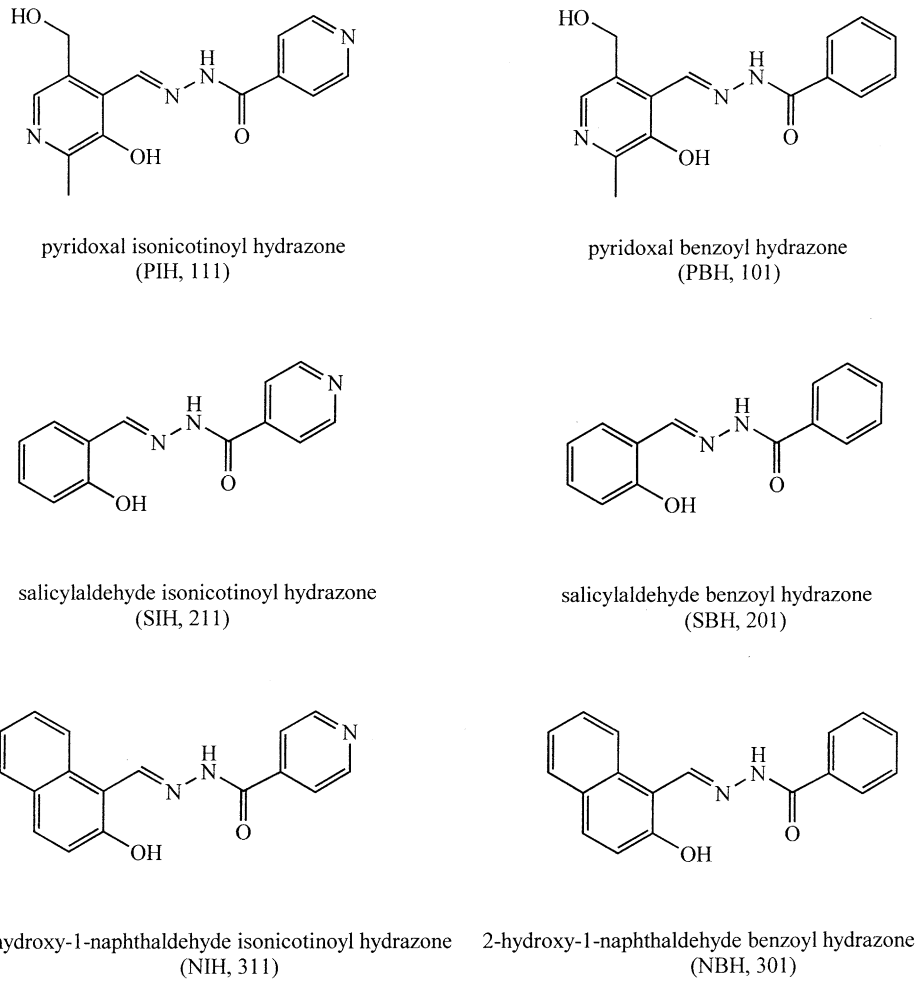

Fig. 1. Structures of the chelators examined. Numerical identifiers as used in previous publications (e.g. [10]) and abbreviations are included.

overload. More recently, over 40 analogs of PIH were synthesized, some of which proved more potent in mobilizing ^{59}Fe from ^{59}Fe-labeled cells [7], including pyridoxal *para*-methoxybenzoyl hydrazone, pyridoxal *meta*-chlorobenzoyl hydrazone (*meta*-ClPBH), and pyridoxal *meta*-fluorobenzoyl hydrazone (*meta*-FPBH). These chelators significantly enhanced biliary excretion of iron in rats following intraperitoneal or oral administration [8]. Since halogenated analogs of PBH (Fig. 1) mobilize iron more efficiently than PIH, the present study was designed to examine the structure–activity relationships among positional isomers of these chelators. The *ortho*, *meta*, and *para* isomers of fluoro-, chloro-, bromo-, and iodo-PBH were synthesized, and their capacities to chelate and efflux ^{59}Fe was examined using reticulocytes in which the non-heme iron pool was labeled with ^{59}Fe. Although reticulocytes are not a target for chelators in the treatment of iron overload, this model is useful for studying the effect of chelators on non-heme, non-ferritin iron, and to assess the capacities of chelators and their iron complexes to cross cell membranes [9].

The experiments presented in this study show that all halogenated PBH analogs chelated similar amounts of ^{59}Fe as demonstrated by increases in both effluxed and intracellular chelator-bound ^{59}Fe. Interestingly, the *ortho*-substituted analogs effluxed more ^{59}Fe, while ^{59}Fe–chelator complexes of the *meta* and *para* analogs were poorly released from cells. In the presence of BSA, release of intracellular ^{59}Fe–chelator was enhanced, such that the *meta* and *para* analogs were as efficient as the *ortho* analogs. Iron complexes of *meta*- and *para*-substituted analogs had high affinity for erythrocyte ghosts, which supports the hypothesis that the release of the complexes is limited by their high affinities for membranes. This study identifies new, highly effective iron–chelators, and demonstrates that efficient release of the iron–chelator from cells is critical in the process of iron mobilization by this series of chelators.

2. Materials and methods

2.1. Chemicals

Pyridoxal hydrochloride, BSA, human apotransferrin, and succinylacetone were purchased from Sigma. Salicylaldehyde and 2-hydroxy-1-naphthaldehyde were purchased

Table 1
Abbreviations of hydrazones synthesized from aromatic aldehydes and halogenated benzoyl hydrazides

	Aldehyde	
Hydrazide	Pyridoxal	Salicylaldehyde
Chlorobenzoyl	ClPBH (*meta* isomer is 108)[a]	ClSBH (*meta* isomer is 208)
Fluorobenzoyl	FPBH (*meta* isomer is 109)	FSBH (*meta* isomer is 209)
Bromobenzoyl	BrPBH (*meta* isomer is 110)	BrSBH (*meta* isomer is 210)
Iodobenzoyl	IPBH	ISBH

[a] Numerical identifiers of analogs, as used in previous studies (e.g. [10]) are included.

from Aldrich. Isonicotinic acid hydrazide and benzoyl hydrazide were purchased from Lancaster. The halogenated benzoyl hydrazides used for preparation of the hydrazones were purchased from Transworld Chemicals. $^{59}FeCl_3$ was purchased from Amersham. Minimum essential medium (MEM) and fetal bovine serum (FBS) were from Gibco. All other chemicals were of the highest quality available.

2.2. Preparation of hydrazone chelators

PIH and its analogs, the structures of which are described in Fig. 1 and Table 1, were synthesized by Schiff base condensation as previously described [10], and the absence of significant amounts of the starting materials in these preparations was confirmed by analytical thin-layer chromatography. The identity and purity of the hydrazones were confirmed by ^{1}H- and ^{13}C-NMR. ^{1}H spectra were similar to those reported previously [10], and a table of ^{1}H chemical shifts is available as supplementary material.[1] Stock solutions of the chelators were prepared in 0.1 M NaOH in 50% aqueous ethanol, and were used immediately, to prevent their base-catalyzed hydrolysis. Control experiments in which stock solutions were prepared in dimethyl sulfoxide yielded similar results (not shown), indicating that any hydrolysis that occurred in the basic solutions was negligible.

2.3. Preparation of ^{59}Fe-labeled reticulocytes

Reticulocytosis was induced in CD1 mice by intraperitoneal injection of 50 mg/kg of phenylhydrazine hydrochloride on 3 consecutive days. Blood was collected 2 or 3 days after the last injection, using heparin as an anticoagulant. Reticulocytes were labeled with ^{59}Fe in the non-heme iron pool by incubating a 30% cell suspension in 1 mM succinylacetone, which inhibits the biosynthesis of protoporphyrin IX, at 37° for 15 min. Then, 10 μM $^{59}Fe_2$-transferrin prepared as previously described [9] was added, and cells were incubated for a further 60 min and washed [9]. These cells accumulate non-heme ^{59}Fe in the mitochondria [9,11], and are designated "^{59}Fe-reticulocytes."

Generally, within each experiment, variability among identically prepared samples is extremely low. Variability among experiments is somewhat greater, probably due to non-uniform levels of non-heme ^{59}Fe in various reticulocyte preparations. To assess the variability among experiments, PIH was used as a control in each experiment to establish reproducibility [9]. Since the effect of PIH was similar in all experiments in this study, quantitative comparisons among the experiments can be made safely.

2.4. ^{59}Fe mobilization from ^{59}Fe-reticulocytes

Approximately 50 μL packed ^{59}Fe-reticulocytes were incubated in 500 μL MEM at 37° in the presence or absence of chelators as described for each experiment. Reticulocytes were pelleted by centrifugation at 210 *g* for 5 min at 4°. Ethanol-soluble cytosolic fractions, which contain ^{59}Fe bound to low-molecular-weight cellular ligands and chelators, were separated from ethanol-insoluble material by lysing the reticulocytes with 200 μL cold double-distilled water, adding 1 mL ethanol, and centrifuging at 630 *g* for 10 min at 4° [9].

2.5. Preparation of murine erythrocyte ghosts

Blood (10 mL) was collected from eight mice, washed five times in 40 mL of 10 mM HEPES containing 150 mM NaCl, pH 7.4, lysed in 40 mL of 5 mM HEPES, pH 8.0 [12], and centrifuged at 20,000 *g* for 20 min at 4°.

2.6. Preparation of $Fe^{3+}(chelator)_2$ complexes

Stock solutions of the chelators were prepared in dimethyl sulfoxide. A stock solution of 5 mM $FeCl_3$ in 100 mM sodium citrate was prepared. Solutions containing Fe^{3+}-citrate and chelator in a 1:2 molar ratio were prepared in PBS in the presence or absence of 1% BSA, and incubated at room temperature for 1 hr, which has been determined spectrophotometrically to be sufficient time for complete complex formation (data not shown). In the absence of BSA, some complexes precipitated; these were centrifuged at 10,000 *g* for 1 min at room temperature prior to their use in the experiment to determine the affinity of the complexes for erythrocyte ghosts, and the final concentrations of iron–chelator complexes were determined.

2.7. Binding of chelators and their Fe^{3+} complexes to BSA

The affinity constants of BSA with ligands were determined spectrophotmetrically in PBS at 37° since the absorption spectra of the chelators and their Fe^{3+} complexes change upon binding BSA. This change in absorbance was measured for each ligand, and the wavelength at

[1] This supplementary material can be obtained by contacting the authors.

which the difference was maximal (380–455 nm) was used for analysis. Data were collected at 10 μM ligand with various concentrations of BSA, since the solubility of some of the ligands is low. Also, the absorbance of some ligands does not increase linearly with concentration over the range necessary for characterization of their binding to BSA by variation of [chelator]. All ligands formed complexes with BSA within 10 sec of the addition of the protein, except PIH and *meta*-BrPBH, which required a 24-hr and a 20-min incubation, respectively, to reach equilibrium. Data were analyzed using Sigmaplot, version 3 for Windows.

3. Results

3.1. Mobilization of ^{59}Fe from reticulocytes by PIH analogs

Reticulocytes in which heme synthesis was inhibited by succinylacetone were labeled with ^{59}Fe by incubation for 60 min with $^{59}Fe_2$-transferrin, followed by incubation with chelators for 2 hr as described in "Section 2." This *in vitro* model, in which cells have a relatively large pool of non-heme iron, has been used successfully to study the effects of PIH and its analogs [7,9,11,13]. When ^{59}Fe-reticulocytes were washed and incubated for 2 hr in MEM in the absence of chelators, approximately 1% of the ^{59}Fe was released into the medium (Fig. 2), probably due to release of a small amount of $^{59}Fe_2$-transferrin from which ^{59}Fe was not dissociated during the labeling period.

^{59}Fe release from ^{59}Fe-labeled reticulocytes into the incubation medium is concentration-dependent and saturable for the chloro- and fluoro-substituted pyridoxal benzoyl hydrazone analogs (Fig. 2). This has been demonstrated previously with pyridoxal isonicotinoyl hydrazone (PIH) [9,13], although its effect was linear over the lower concentration range examined in this study. The concentration of pyridoxal chlorobenzoyl hydrazone (ClPBH) causing half-maximal ^{59}Fe release was approximately 15 μM for all positional isomers, while the maximal release was much greater for *ortho*-ClPBH than for the *meta* and *para* isomers (Fig. 2A). In contrast, the three pyridoxal fluorobenzoyl hydrazone (FPBH) isomers had similar capacities to release ^{59}Fe in this model (Fig. 2B). It is worth noting that *ortho*-ClPBH and all FPBH isomers released significant amounts of iron at micromolar concentrations, which may be expected to be therapeutically achievable.

It can be seen from the concentration-dependence experiments that the choice of chelator concentration in this assay may have a significant effect on the results of a structure–activity relationship study, since the relative effectiveness of the chelators depended on the concentration at which the experiments were performed. As all analogs except PIH exhibited maximal activity at 100 μM (Fig. 2), this concentration was chosen for subsequent experiments.

The kinetics of ^{59}Fe mobilization by ClPBH isomers and PIH were examined (Fig. 3). In addition to measuring the release of ^{59}Fe into the incubation medium, radioactivity in the ethanol-soluble and -insoluble intracellular fractions was determined, as described in "Section 2." In the absence of chelator treatment, nearly all intracellular radioactivity is found in the ethanol-insoluble fraction, which corresponds to ^{59}Fe bound to proteins, membranes, and inside organelles, including mitochondria. With this method of analysis, both the amounts of ^{59}Fe released from cells into the incubation medium by the chelators as well as the total amount of ^{59}Fe bound to the chelators (i.e. the sum of the radioactivity found in the incubation medium and the ethanol-soluble fraction) can be determined in the same experiment.

The kinetics of ^{59}Fe binding to the chelators were similar for all analogs examined under these conditions (Fig. 3), and were dependent on both the capacity of the chelators to bind intracellular iron and the membrane permeability of the iron–chelator complexes. The kinetics of the combined

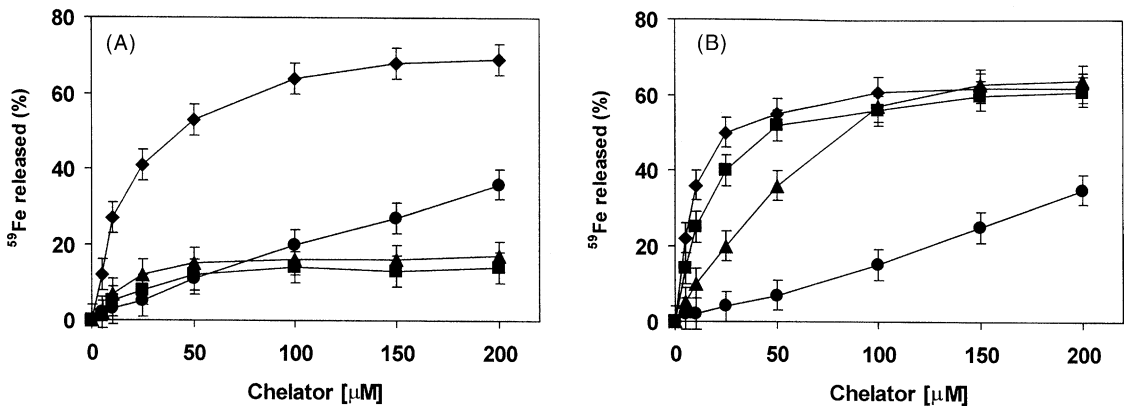

Fig. 2. Concentration dependence of ^{59}Fe release from ^{59}Fe-reticulocytes by ClPBH (A) and FPBH (B) isomers. Cells were incubated with the chelators for 2 hr, and the percentage of ^{59}Fe released into the incubation medium was determined at each concentration. Error bars represent standard deviations of triplicate measurements. Key: (◆) *ortho* isomer, (■) *meta* isomer, (▲) *para* isomer, and (●) PIH.

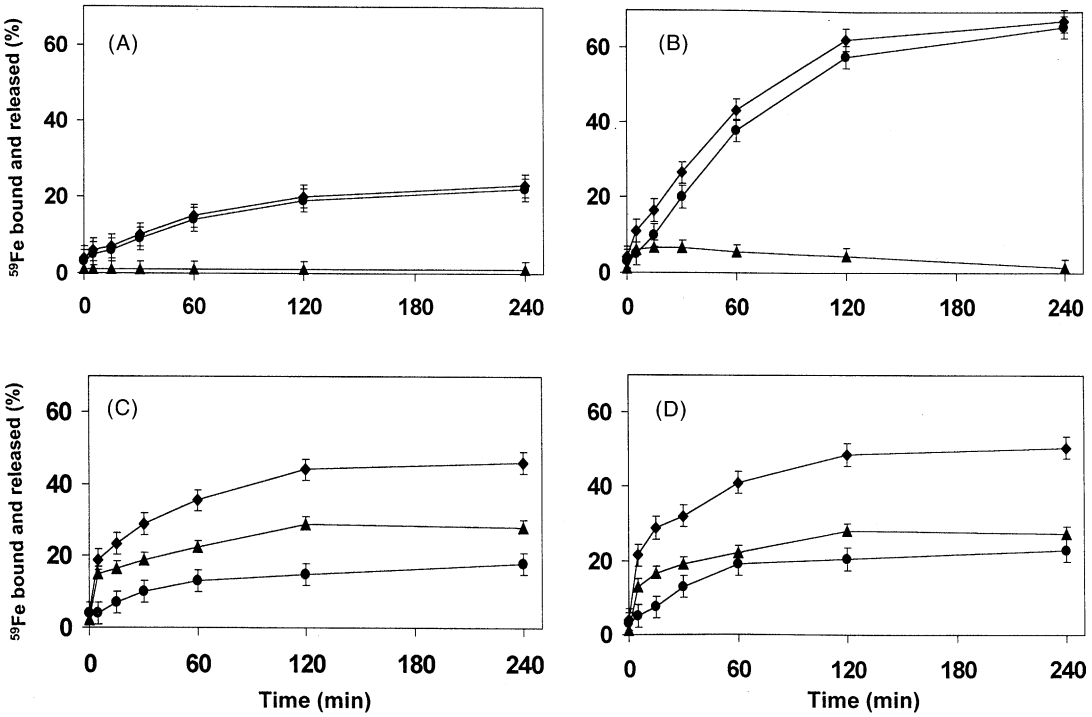

Fig. 3. Kinetics of ^{59}Fe binding and release from ^{59}Fe-reticulocytes by 100 μM PIH (A), *o*-ClPBH (B), *m*-ClPBH (C), and *p*-ClPBH (D). Error bars represent standard deviations of triplicate measurements. Key: (◆) total ^{59}Fe bound (i.e. the sum of ethanol-soluble and released ^{59}Fe), (●) ^{59}Fe released into the incubation medium, and (▲) intracellular ethanol-soluble ^{59}Fe.

steps of entering the cell and accessing iron were approximately the same for all chelators (Fig. 3). Therefore, these steps are not involved in the observed structure–activity relationships. It has been hypothesized that membrane permeability is not rate-limiting in terms of iron mobilization by PIH, due to its rapid entry into cells [9].

Although it has not been determined unequivocally that the iron–chelator complex is the species present in the cytosol, nor that it is the species released from the cell, there is evidence to suggest that both of these assumptions are reasonable. Since ^{59}Fe-labeled, untreated reticulocytes contain very little ethanol-soluble radioactivity, it can be concluded that the cellular ligands involved in chelating the labeled iron are not ethanol-soluble. Since treatment of reticulocytes with chelators causes increases in ethanol-soluble radioactivity, it is reasonable to assume that this represents iron–chelator. Also, the simplest explanation of the different rates of release of radioactivity observed in Fig. 3 is that the iron–chelator complex is the species released, though it cannot be excluded that iron could be transferred from the chelator to a cellular iron ligand in a rate-determining manner, which is then released.

For PIH and *ortho*-ClPBH, the iron binding and release curves were almost identical (Fig. 3A and B), indicating that the iron–chelator complex is released from the cell almost as fast as it is produced, and that very little accumulates in the cytosol. For *meta*- and *para*-ClPBH (Fig. 3C and D), ^{59}Fe release lagged behind ^{59}Fe binding, and significant amounts of ^{59}Fe, presumably as its chelator complex, accumulated in the cytosol. The main difference in the kinetics of ^{59}Fe mobilization among these analogs was in the rate at which the respective ^{59}Fe complexes were released from the cell.

A screen of the capacities of the series of PIH and SIH analogs was undertaken. For all analogs except PIH, approximately 45–60% of the total ^{59}Fe was chelator-bound (Fig. 4). The observed differences in the amount of ^{59}Fe released from the cells depended not upon the amount of ^{59}Fe bound, but rather upon the release of ^{59}Fe–chelator. The position of the halogen on the aromatic ring was apparently more important than whether it was a chloro, bromo, or iodo substituent. Some analogs (mainly the *meta* and *para* isomers) caused significant accumulation of ^{59}Fe in the ethanol-soluble fraction. Only among the FPBH analogs did all three positional isomers release most of the ^{59}Fe bound. The analogous series of compounds synthesized from 2-hydroxy-1-naphthaldehyde was also screened (data not shown). Due to the toxicity of these compounds, which resulted in hemolysis, the chelator concentration in these experiments was reduced to 25 μM. All chelators in this series bound intracellular ^{59}Fe, but were poorly released from the cells.

All the analogs examined in Fig. 4 except for PIH bound approximately the same amount of ^{59}Fe in the reticulocyte model, even though large differences in the affinity of these analogs for Fe^{3+} have been reported [14]. It appears that there is a pool of ^{59}Fe in the reticulocytes that is unavailable to any of the chelators. Although little is known about the nature of this iron pool, it is unlikely that there is significant heme-associated ^{59}Fe in this model, due to

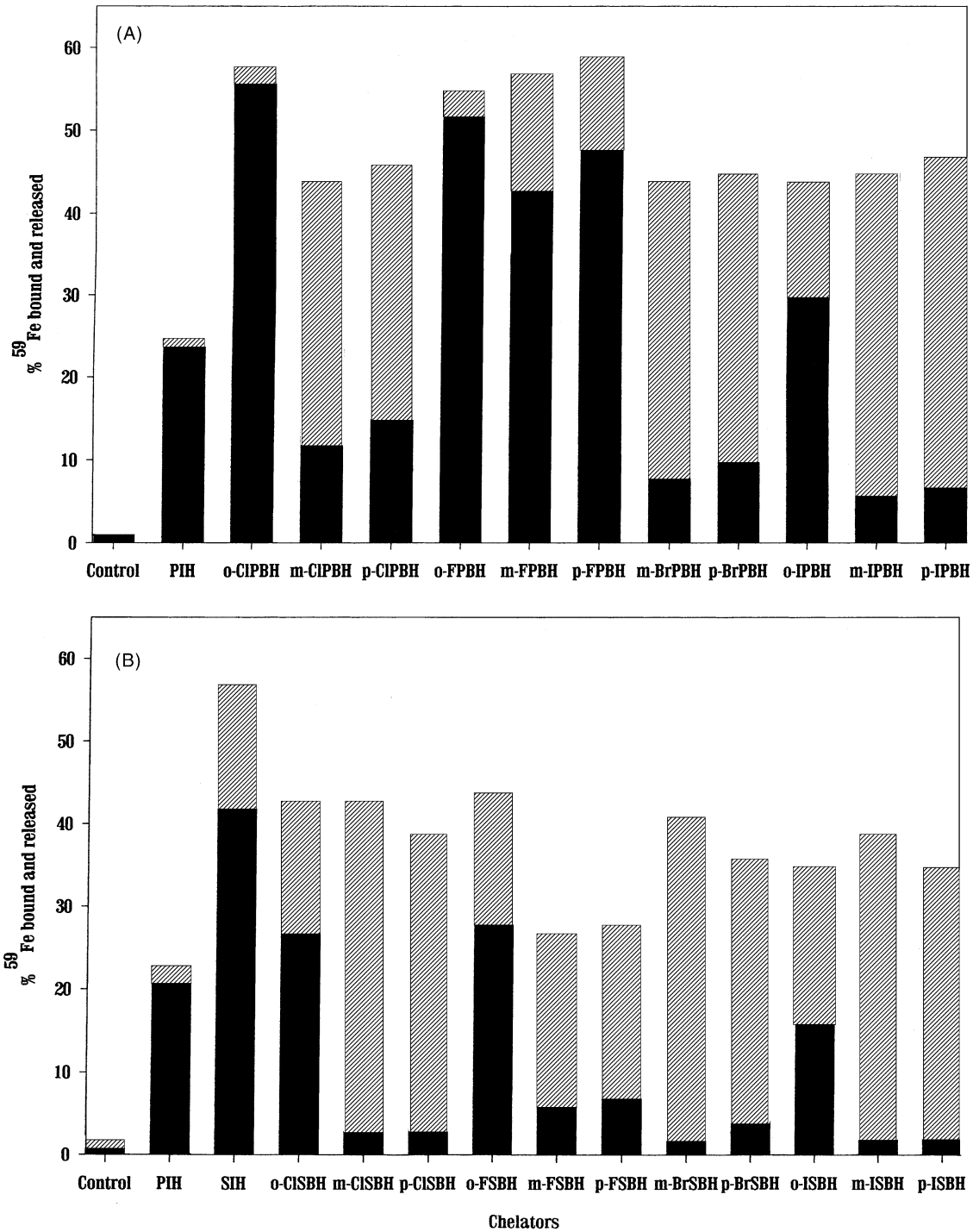

Fig. 4. ^{59}Fe binding and release from ^{59}Fe-reticulocytes by 100 μM chelators synthesized from pyridoxal (A) and salicylaldehyde (B). Key: (black bars) ^{59}Fe released into the incubation medium; and (hatched bars) intracellular ethanol-soluble ^{59}Fe. Standard deviations did not exceed 4%. Results shown are from a single experiment, which was performed six times.

effective inhibition of protoporphyrin IX synthesis by succinylacetone [9].

3.2. *^{59}Fe mobilization by PIH analogs in the presence of BSA*

The preceding experiments were performed in the absence of FBS and BSA for comparison with previous studies [7,15–17]. BSA had a concentration-dependent effect on the capacity of ClPBH analogs to bind intracellular ^{59}Fe, but its effect on the activity of PIH was insignificant (Fig. 5). As [BSA] increased, the amount of ^{59}Fe bound by *ortho*-ClPBH gradually decreased. Since BSA remains in the extracellular space, the most likely explanation for this effect is that BSA reduces the delivery of the chelator to the cell. This effect was also observed at higher

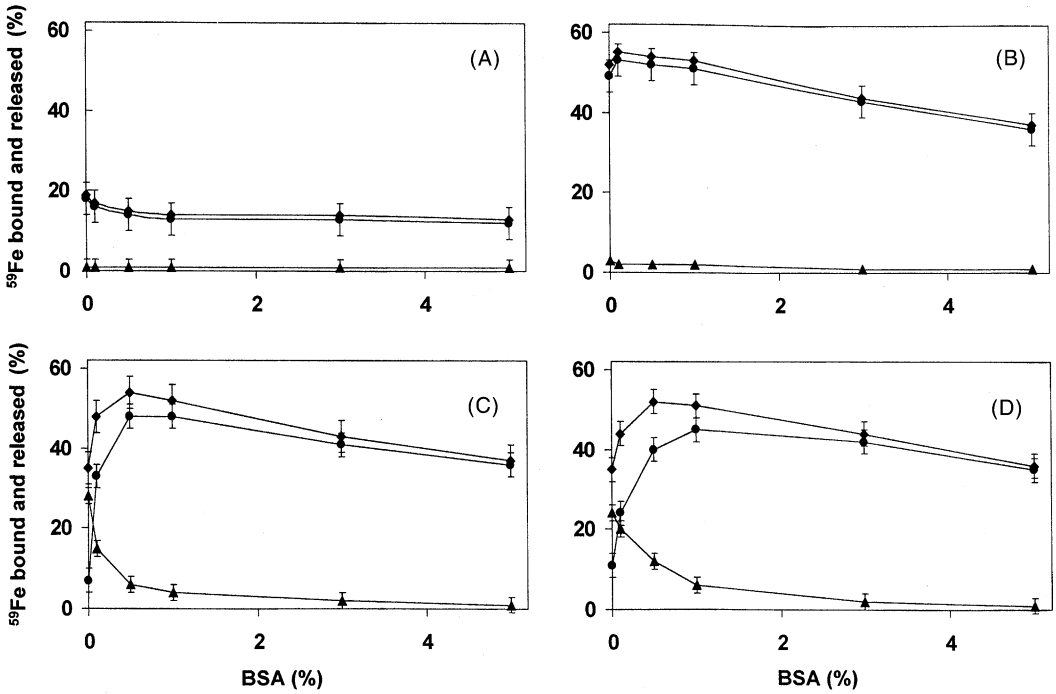

Fig. 5. Dependence of ^{59}Fe binding and release from ^{59}Fe-reticulocytes by 100 μM PIH (A), *o*-ClPBH (B), *m*-ClPBH (C), and *p*-ClPBH (D) on the concentration of BSA in the incubation medium. Error bars represent standard deviations of triplicate measurements. Key: (◆) total ^{59}Fe bound (i.e. the sum of ethanol-soluble and released ^{59}Fe), (●)^{59}Fe released into the incubation medium, and (▲) intracellular ethanol-soluble ^{59}Fe.

concentrations of BSA for the *meta*- and *para*-ClPBH isomers, although at lower concentrations, ^{59}Fe binding to the chelators was increased.

The most significant effect of BSA on the action of the chelators, however, was the large concentration-dependent increase in the fraction of ^{59}Fe–chelator released from the cells by *meta*- and *para*-ClPBH (Fig. 5C and D), which had significant effects on the levels of cytosolic ^{59}Fe accumulation observed. Since ^{59}Fe is efficiently released from cells by PIH and *ortho*-ClPBH, no effects of BSA on ^{59}Fe release were observed for these analogs (Fig. 5A and B).

BSA at a concentration of 1% had no effect on the kinetics of ^{59}Fe binding by either PIH or the ClPBH analogs (compare Figs. 3 and 6). Since cytosolic accumulation of ethanol-soluble radioactivity induced by *meta*- and *para*-ClPBH was greatly reduced in the presence of BSA, it can be concluded that the rates of release of ^{59}Fe by these analogs were increased such that they cause ^{59}Fe to be released from cells nearly as quickly as it was bound.

To determine whether the effects of BSA on the ClPBH isomers were characteristic of the whole series of halogenated analogs, ^{59}Fe-reticulocytes were incubated with 1% BSA and 100 μM chelators (Fig. 7), in an experiment analogous to that of Fig. 4. Small differences were observed in the total amounts of ^{59}Fe bound by these analogs compared to values in the absence of BSA (Fig. 4), suggesting that BSA may have affected the effective chelator concentration, as observed for the ClPBH isomers (Fig. 5). No significant differences in ^{59}Fe release from reticulocytes were observed for the analogs, which export ^{59}Fe efficiently in the absence of BSA. Cytosolic accumulation of ^{59}Fe by the *meta*- and *para*-substituted analogs, which cause ^{59}Fe to be released slowly (Fig. 4), was reduced significantly in the presence of BSA, presumably by the same kinetic effect observed for the ClPBH isomers (Fig. 6). Thus, the importance of the position of the halogen substituent on the efficacy of ^{59}Fe release from reticulocytes, as observed for the ClPBH isomers (Fig. 2A), seems to be a general feature of ^{59}Fe mobilization by all halogenated analogs.

3.3. Mechanism of ^{59}Fe binding and release by PIH analogs

Complexes of PIH analogs with Fe^{3+} are known to be lipophilic [16,18]. If transport of the chelates out of the cell is the rate-determining step for release of ^{59}Fe from reticulocytes as shown in Fig. 4, it may be due to high affinity of the complexes for a lipophilic environment such as the cell membrane.

$^{59}Fe^{3+}(chelator)_2$ complexes of the halogenated analogs were prepared as described in "Section 2," and incubated in PBS with erythrocyte ghosts for 2 hr. Due to the low solubility of some of the complexes, the final concentration used in the incubation with erythrocyte ghosts varied in this experiment as described (Table 2), and binding of the complexes to ghosts can be evaluated only qualitatively. Complexes that were released slowly from the reticulocytes (Figs. 3 and 4) had high affinity for ghosts (Table 2). This supports the hypothesis that release of the complexes from cells is kinetically limited by their high affinities for

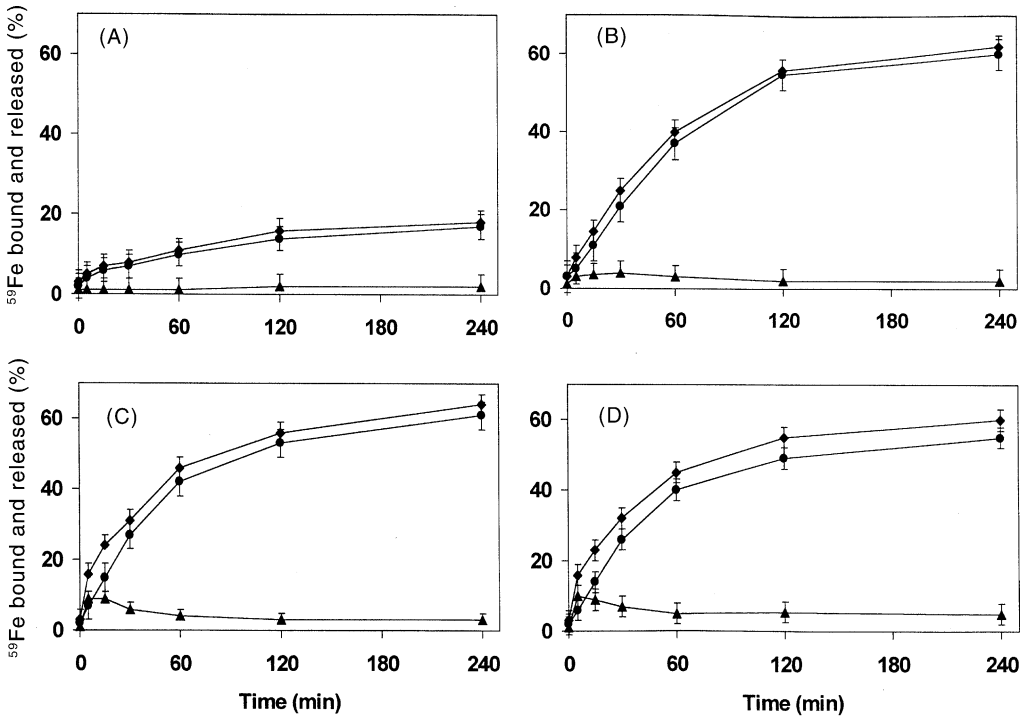

Fig. 6. Kinetics of ^{59}Fe binding and release from ^{59}Fe-reticulocytes by 100 μM PIH (A), *o*-ClPBH (B), *m*-ClPBH (C), and *p*-ClPBH (D) in the presence of 1% BSA. Error bars represent standard deviations of triplicate measurements. Key: (◆) total ^{59}Fe bound (i.e. the sum of ethanol-soluble and released ^{59}Fe), (●) ^{59}Fe released into the incubation medium, and (▲) intracellular ethanol-soluble ^{59}Fe.

membranes, although it is also possible that the complexes could bind some intracellular macromolecules or low-molecular-weight ligands, shifting the equilibrium toward intracellular accumulation of ^{59}Fe. The complexes that were released slowly were also those that precipitated at 25 μM (and are thus presumably the most lipophilic), which is further evidence for lipophilicity as the feature determining release rates.

Direct interaction of BSA with the chelators and their Fe^{3+} complexes is sufficient to explain all of the observed effects of BSA in the preceding experiments. Binding of extracellular $Fe^{3+}(chelator)_2$ may change the kinetic and/or thermodynamic characteristics of iron mobilization. The affinity of BSA for ligands (i.e. the chelators and their Fe^{3+} complexes) was examined spectrophotometrically at 10 μM ligand. Spectral changes occurred over the wavelength range 300–450 nm upon binding of the ligands to BSA. By comparison of the spectra of the protein-bound complexes to those of the free chelator, it was concluded that the complexes did not dissociate upon

Table 2
Binding of Fe–chelator complexes to erythrocyte ghosts[a]

	PBS		1% BSA	
	[Fe–chelator$_2$] (μM)[b]	nmol/5 × 10^{11} ghosts	[Fe–chelator$_2$] (μM)	nmol/5 × 10^{11} ghosts
Control	20 ± 0.1	89 ± 2	20 ± 0.2	110 ± 2
o-ClPBH	20 ± 0.5	100 ± 10	20 ± 0.2	60 ± 15
m-ClPBH	20 ± 0.4	1030 ± 10	20 ± 0.1	110 ± 10
p-ClPBH	19 ± 0.2	820 ± 30	20 ± 0.2	190 ± 10
o-FPBH	19 ± 0.1	111 ± 4	20 ± 0.3	100 ± 20
m-FPBH	20 ± 0.3	190 ± 10	20 ± 0.2	90 ± 15
p-FPBH	19 ± 0.1	210 ± 30	20 ± 0.1	110 ± 20
m-BrPBH	19 ± 0.1	1100 ± 100	20 ± 0.2	100 ± 10
p-BrPBH	12 ± 0.1	1340 ± 50	20 ± 0.2	140 ± 10
o-IPBH	5 ± 0.2	150 ± 20	20 ± 0.3	100 ± 10
m-IPBH	19 ± 0.2	430 ± 20	20 ± 0.1	90 ± 10
p-IPBH	6 ± 0.1	390 ± 20	20 ± 0.2	190 ± 20
PIH	5 ± 0.2	70 ± 20	20 ± 0.1	100 ± 10

[a] Values are means ± SD (N = 3).
[b] Due to insolubility of some Fe–chelator$_2$ complexes in the absence of BSA, the concentration of complex incubated with ghosts varies.

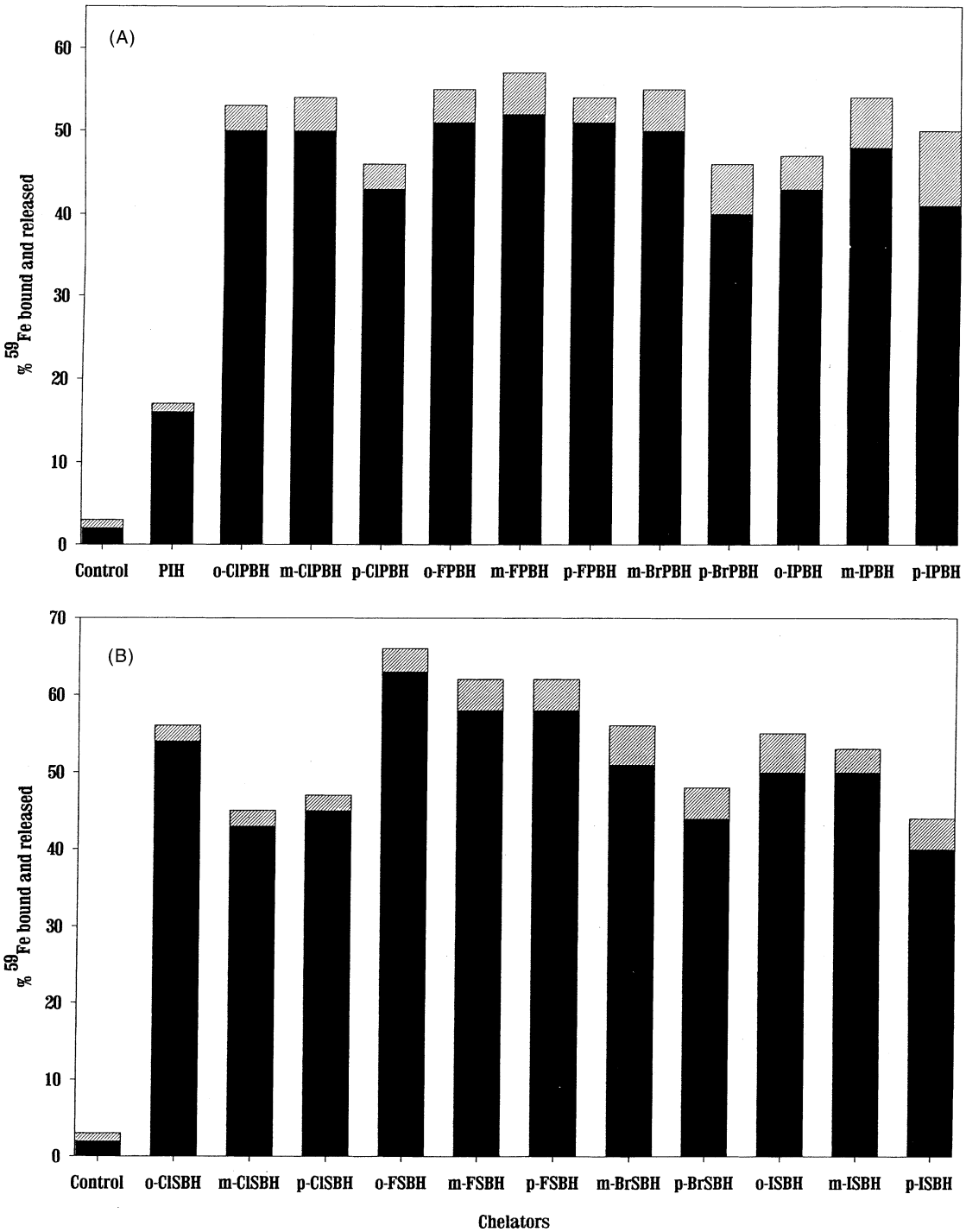

Fig. 7. ^{59}Fe binding and release from ^{59}Fe-reticulocytes in the presence of 1% BSA by 100 μM chelators synthesized from pyridoxal (A) and salicylaldehyde (B). Key: (black bars) ^{59}Fe released into the incubation medium; and (hatched bars) intracellular ethanol-soluble ^{59}Fe. Standard deviations did not exceed 4%. Results shown are from a single experiment, which was performed four times.

binding BSA. Difference spectra (A_{Diff}), shown in Fig. 8A for *meta*-FPBH and its Fe^{3+} complex, were calculated as follows:

$$A_{Diff} = A_{BSA+ligand} - (A_{BSA} + A_{ligand}) \quad (1)$$

in which A is the absorbance spectrum of the subscripted species. Binding of ligands to BSA was analyzed at various concentrations of BSA ($[BSA]_{Tot}$) at the wavelength at which A_{Diff} was maximal. The amplitude of A_{Diff} when the ligand was completely bound to BSA, A_{Diff}MAX, was determined by an unweighted, least-squares fit of the data to a saturation equation, shown for *m*-FPBH and its Fe^{3+} complex in Fig. 8B:

$$A_{Diff} = \frac{A_{Diff}MAX[ligand]}{[ligand] + K} \quad (2)$$

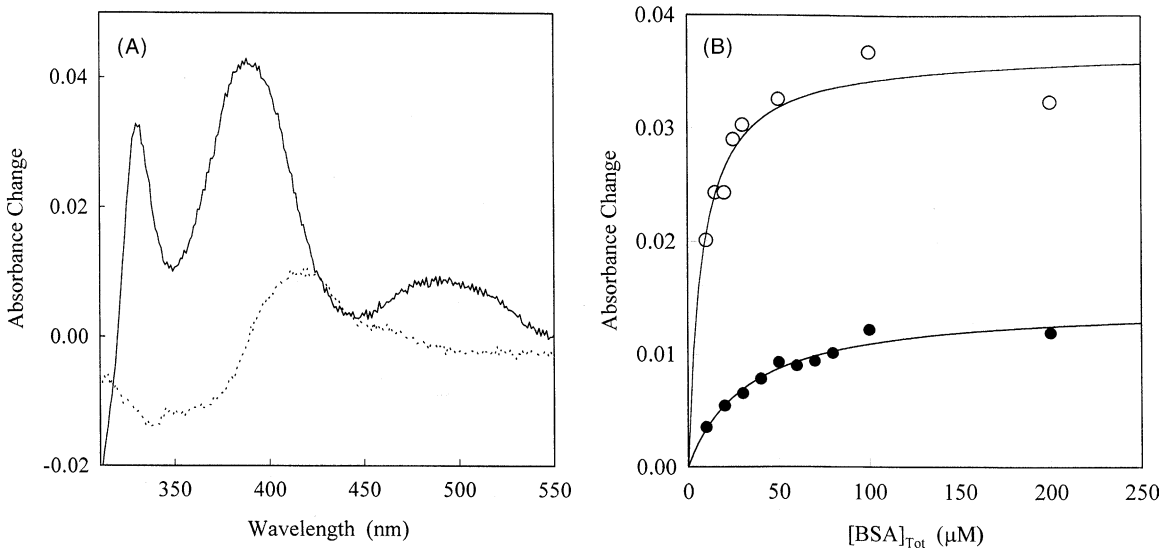

Fig. 8. Binding of ligands to BSA. (A) Difference spectra as calculated from Eq. (1) for *m*-FPBH (dotted line) and its Fe^{3+} complex (solid line). (B) Dependence of the absorbance changes at 420 and 390 nm for *m*-FPBH (●) and its Fe^{3+} complex (○), respectively, on $[BSA]_{Tot}$. Solid lines represent fits of the data to Eq. (2). Results shown are from a single experiment, which was performed twice.

$A_{Diff}MAX$ was used to calculate [BSA − *L*], the concentration of ligand bound to BSA at each $[BSA]_{Tot}$. The binding constant describing the affinity of the ligand for BSA, K_a, was determined by fitting [BSA − *L*] and $[BSA]_{Tot}$ to the following indirectly defined function:

$$K_a = \frac{[BSA - L]}{(10 - [BSA - L])([BSA]_{Tot} - [BSA - L])} \quad (3)$$

Values of K_a for the chelators and their Fe^{3+} complexes are reported in Table 3.

All chelators tested, and their Fe^{3+} complexes, bound BSA, regardless of the position of the halogen. In addition to the high-affinity binding of $Fe^{3+}(chelator)_2$ complexes characterized, a second lower-affinity binding was observed when the concentration of the complex exceeded that of BSA. Since conditions under which the second site on the protein is occupied are unlikely to occur either *in vivo* or *in vitro*, binding of the complexes to this site were not investigated further. Binding to the high-affinity site was determined under conditions such that the second site was not occupied.

Table 3
Affinity constants of BSA–chelator and BSA–$(Fe^{3+}(chelator)_2)$[a]

	Chelalor K_a (M^{-1})	$Fe^{3+}(chelator)_2$ K_a (M^{-1})
PBH	34,000 ± 4,000	180,000 ± 90,000
o-ClPBH	13,300 ± 400	70,000 ± 7,000
m-ClPBH	140,000 ± 20,000	>500,000[b]
p-ClPBH	81,000 ± 10,000	ND[c]
o-FPBH	26,000 ± 2,000	26,800 ± 1,300
m-FPBH	36,000 ± 3,000	180,000 ± 30,000
p-FPBH	63,000 ± 13,000	170,000 ± 20,000
m-BrPBH	37,000 ± 10,000	>500,000[b]
p-BrPBH	61,000 ± 6,000	ND[c]
PIH	72,000 ± 5,000	7,000 ± 800

[a] Experiments were performed twice. Errors are fitting errors from Eq. (3).
[b] Affinity was too high to measure spectrophotometrically.
[c] Not determined due to low solubility of the $Fe^{3+}(chelator)_2$ complex.

Binding of chelators and their Fe^{3+} complexes to BSA is likely the cause of the effects of this protein on the capacity of the chelators to bind intracellular ^{59}Fe, as shown in Figs. 5–7. The BSA–chelator complex is formed too quickly for the kinetics to be followed spectrophotometrically for all chelators except PIH and *m*-BrPBH. The binding of the Fe^{3+} complexes of the chelators was of higher affinity than that of the free chelator in each case (Table 3), which is consistent with the observation that the complexes are generally more lipophilic than the free ligands [19]. At high concentrations of BSA, binding of the chelators limits the concentration of chelator available for entering the cell, as shown in Fig. 5. The apparent increase in chelator delivery to cells at lower [BSA], indirectly detected by the increase in ^{59}Fe binding by *meta*- and *para*-ClPBH observed in panels C and D of Fig. 5, was similar to the effect of this protein on uptake of fatty acids by hepatocytes [20]. It may be that, the BSA–chelator complex reduces the diffusional barrier to the membrane surface, where it spontaneously dissociates in response to locally low chelator concentrations, thus maintaining the gradient that drives diffusion of the ligand into the cell.

4. Discussion

The development of effective, orally available iron–chelators is a subject of continuing interest for the treatment of secondary iron overload, including that caused by

the chronic blood transfusions required by β-thalassemic patients. Early studies [5,21] identified PIH as a candidate worthy of further attention, and *in vitro* [9,13] and *in vivo* [8] studies have demonstrated that halogenated PBH analogs (structures described in Fig. 1 and Table 1) are more effective at mobilizing cellular iron than the parent compound. In this study, positional isomers of these analogs were examined in the ongoing effort to elucidate the mechanism of action of these chelators. Among the chelators in this study, the most significant factor in determining overall efficacy was the position of the halogen on the aromatic ring of the hydrazide moiety, and, therefore, the rate of release of the iron complexes from the cells. The *ortho*-substituted analogs were the most effective *in vitro*, and deserve further attention as potentially effective drugs *in vivo*.

4.1. Structure–activity relationships describing ^{59}Fe mobilization by PIH analogs

Many investigations have been undertaken to examine structure–activity relationships defining the activity of PIH-related chelators [7,8,16,22–24], and although the importance of lipophilicity has been reported previously [16,23], no clear correlation with chelation efficiency has been identified. The small structural variations among the chelators in this study allowed identification of the features governing the individual steps in the mechanism of chelation of intracellular iron, the most significant of which was the position of the halogen substituent on the benzene ring. For the first time in a structure–activity study, both ^{59}Fe binding and release of the complexes from cells were assessed, allowing the comparison of ^{59}Fe binding efficiencies of the chelators as well as ^{59}Fe release rates. ^{59}Fe release from reticulocytes was the primary determinant of chelator efficiency in this series of chelators (Fig. 4).

Significant differences in the capacities of PIH analogs to release ^{59}Fe from cells were observed (Fig. 4), which appear to be due to the membrane permeability of the Fe^{3+} complexes (Fig. 3 and Table 2). The ethyl acetate/water partition coefficients have been measured for some of the pyridoxal- and salicylaldehyde-based chelators and their Fe^{3+} complexes [19]. These values demonstrate the much higher lipophilicity of *meta*-ClPBH and *meta*-BrPBH as compared to *meta*-FPBH, PBH, and PIH, which corresponds to the rates of release of the ^{59}Fe complexes from reticulocytes (relatively slowly or quickly, respectively). This correlation provides additional evidence that the structural variations investigated in this study affect the lipophilicity of the chelators, and especially of their Fe^{3+} complexes, which cause the observed differences in ^{59}Fe release. The effects of these substituents on lipophilicity are unclear, but they do not appear to be due to electronic effects, in which case the magnitude of the effects should decrease in the order F > Cl > Br > I > H. It may be that the subsitituent effects are in part steric, as the presence of the fluoro substituent, which had little effect on the rate of release of ^{59}Fe from reticulocytes regardless of its position on the aromatic ring (Fig. 4), has nearly the same radius as the hydrogen atom, while the other halogen substituents are substantially larger.

The kinetics of ^{59}Fe mobilization by PIH are quite different from a previously reported experiment which was done with 1 mM PIH [13], a concentration 10-fold higher than that used in the experiments shown in Fig. 3A. Significant accumulation of ^{59}FePIH in the cytosol was observed with the higher chelator concentration, indicating that the mechanism by which ^{59}Fe is released from the cell had reached a maximum rate. From the concentration-dependence experiments (Fig. 2), it is evident that the capacity of PIH to bind ^{59}Fe is not limited below 200 μM, in agreement with previous observations [21]. It is likely that a larger quantity of ^{59}FePIH was produced when 1 mM PIH was incubated with ^{59}Fe-reticulocytes, which apparently saturated the release mechanism, while the quantity of ^{59}FePIH produced in the experiment shown in Fig. 2A did not. Thus, the kinetics of ^{59}Fe release, and, as a result, the intracellular accumulation of ^{59}Fe–chelator, can change depending on the concentration of chelator used, which has also been shown for naphthaldehyde isonicotinoyl hydrazone [17].

4.2. Mechanism of release of ^{59}Fe–chelator complexes, and effect of BSA

Since BSA presumably does not enter cells, the effects of the protein on mobilization of ^{59}Fe must occur via modulation of the delivery of the chelators to the cells, which affects intracellular chelator concentrations, and the release of the ^{59}Fe–chelator complexes, which affects intracellular complex concentrations, as measured by ethanol-soluble radioactivity. It is known from previous studies investigating the effect of lipophilicity of PIH analogs on ^{59}Fe mobilization that iron–chelator complexes, and many of the chelators themselves, are lipophilic [19]. Therefore, they may accumulate preferentially in the cell membrane, and not enter the aqueous incubation medium. BSA may provide a sink, due to its affinity for lipophilic species [25] that allows the complexes to leave the membrane, bypassing the apparent kinetic block.

The mechanism by which BSA affects the transport of various species across the cell membrane is unknown. The discovery that other proteins are equally or more efficient at promoting palmitate uptake [19] is evidence against a BSA-receptor-based mechanism. A BSA-induced increase in the efficiency of transport of a species into the cell (as was observed for *meta*- and *para*-ClPBH) may be explained by the spontaneous dissociation of the BSA–ligand complex as the concentration of the free ligand near the membrane decreases due to its diffusion into the cell [20]. In an analogous manner, BSA may promote the release of a species from the cell by binding it as it leaves

the cell membrane, thereby reducing the extracellular concentration of free ligand, inducing increased release of the ligand from the membrane.

The presence of BSA, an extracellular sink for iron–chelator complexes, increased the apparent membrane permeability of the iron–chelator complexes, such that, in the presence of 1% BSA, nearly all ^{59}Fe that was bound by the chelators was released from labeled reticulocytes during the 2-hr incubation (Fig. 7).

BSA is known to bind lipophilic species in plasma, and to affect their metabolism. Extensive binding to serum proteins is consistent with hepatic and biliary excretion, which is the main route of elimination of ^{59}Fe after administration of PIH [6] and its analogs [8]. BSA and possibly other plasma proteins may be involved in removal of iron–chelator complexes from tissues. This feature may be quite important in determining the effectiveness of analogs *in vivo*. While the efficiency of chelation in the presence of BSA was similar for all analogs (Fig. 7), there are significant differences in efficacy among these compounds *in vivo* [8], which may be the result of many pharmacokinetic factors, including bioavailability, the rate of absorption from the gut, plasma half-life, metabolism, and tissue distribution. Furthermore, it must be noted that while albumin is abundant in human serum, it is not in rats, the animal model in which the *in vivo* studies were done [8].

This study has demonstrated the importance of membrane permeability of iron–chelator complexes in the capacity of PIH analogs to mobilize iron. Among chelators with similar abilities to bind iron, the rate of release of the iron–chelator complex may be a major determinant of efficacy *in vivo* as well as *in vitro*. In addition, the *ortho*-substituted halogenated analogs of PBH have been identified as effective chelators *in vitro*; these may be expected to be more effective than their *meta*- and *para*-substituted isomers at iron mobilization *in vivo*.

Acknowledgments

This work was supported by grants from the Canadian Institutes for Health Research (formerly the Medical Research Council of Canada). The authors gratefully acknowledge the assistance of Pat Farrell (Chemistry Department, McGill University) for assistance in interpreting NMR spectra.

References

[1] Gutteridge JM, Halliwell B. Iron toxicity and oxygen radicals. Baillieres Clin Haematol 1989;2:195–256.
[2] Hershko C, Konijn AM, Link G. Iron chelators for thalassaemia. Br J Haematol 1998;101:399–406.
[3] Olivieri NF, Brittenham GM. Iron-chelating therapy and the treatment of thalassemia. Blood 1997;89:739–61.
[4] Summers MR, Jacobs A, Tudway D, Perera P, Ricketts C. Studies in desferrioxamine and ferrioxamine metabolism in normal and iron-loaded subjects. Br J Haematol 1979;42:547–55.
[5] Ponka P, Borova J, Neuwirt J, Fuchs O. Mobilization of iron from reticulocytes. Identification of pyridoxal isonicotinoyl hydrazone as a new iron chelating agent. FEBS Lett 1979;97:317–21.
[6] Cikrt M, Ponka P, Necas E, Neuwirt J. Biliary iron excretion in rats following pyridoxal isonicotinoyl hydrazone. Br J Haematol 1980;45:275–83.
[7] Ponka P, Richardson D, Baker E, Schulman HM, Edward JT. Effect of pyridoxal isonicotinoyl hydrazone and other hydrazones on iron release from macrophages, reticulocytes and hepatocytes. Biochim Biophys Acta 1988;967:122–9.
[8] Blaha K, Cikrt M, Nerudova J, Fornuskova H, Ponka HF. Biliary iron excretion in rats following treatment with analogs of pyridoxal isonicotinoyl hydrazone. Blood 1998;91:4368–72.
[9] Huang AR, Ponka P. A study of the mechanism of action of pyridoxal isonicotinoyl hydrazone at the cellular level using reticulocytes loaded with non-heme ^{59}Fe. Biochim Biophys Acta 1983;757:306–15.
[10] Edward JT, Gauthier M, Chubb FL, Ponka P. Synthesis of new acylhydrazones as iron-chelating compounds. J Chem Eng Data 1988;33:538–40.
[11] Morgan EH. Chelator-mediated iron efflux from reticulocytes. Biochim Biophys Acta 1983;733:39–50.
[12] Cheetham JJ, Nir S, Johnson E, Flanagan TD, Epand RM. The effects of membrane physical properties on the fusion of Sendai virus with human erythrocyte ghosts and liposomes. Analysis of kinetics and extent of fusion. J Biol Chem 1994;269:5467–72.
[13] Ponka P, Grady RW, Wilczynska A, Schulman HM. The effect of various chelating agents on the mobilization of iron from reticulocytes in the presence and absence of pyridoxal isonicotinoyl hydrazone. Biochim Biophys Acta 1984;802:477–89.
[14] Vitolo ML, Hefter GT, Clare BW, Webb J. Iron chelators of the pyridoxal isonicotinoyl hydrazone class. Part II. Formation constants with iron(III) and iron(II). Inorg Chim Acta 1990;170:171–6.
[15] Richardson DR, Ponka P. The iron metabolism of the human neuroblastoma cell: lack of relationship between the efficacy of iron chelation and the inhibition of DNA synthesis. J Lab Clin Med 1994;124:660–71.
[16] Ponka P, Richardson DR, Edward JT, Chubb FL. Iron chelators of the pyridoxal isonicotinoyl hydrazone class. Relationship of the lipophilicity of the apochelator to its ability to mobilise iron from reticulocytes *in vitro*. Can J Physiol Pharmacol 1994;72:659–66.
[17] Richardson DR, Milnes K. The potential of iron chelators of the pyridoxal isonicotinoyl hydrazone class as effective antiproliferative agents II: the mechanism of action of ligands derived from salicylaldehyde benzoyl hydrazone and 2-hydroxy-1-naphthylaldehyde benzoyl hydrazone. Blood 1997;89:3025–38.
[18] Edward JT, Chubb FL, Sangster J. Iron chelators of the pyridoxal isonicotinoyl hydrazone class. Relationship of the lipophilicity of the apochelator to its ability to mobilize iron from reticulocytes *in vitro*: reappraisal of reported partition coefficients. Can J Physiol Pharmacol 1997;75:1362–8.
[19] Edward JT, Ponka P, Richardson DR. Partition coefficients of the iron(III) complexes of pyridoxal isonicotinoyl hydrazone and its analogs and the correlation to iron chelation efficacy. Biometals 1995;8:209–17.
[20] Burczynski FJ, Wang GQ, Hnatowich M. Effect of binding protein surface charge on palmitate uptake by hepatocyte suspensions. Br J Pharmacol 1997;120:1215–20.
[21] Ponka P, Borova J, Neuwirt J, Fuchs O, Necas E. A study of intracellular iron metabolism using pyridoxal isonicotinoyl hydrazone and other synthetic chelating agents. Biochim Biophys Acta 1979;586:278–97.
[22] Baker E, Richardson D, Gross S, Ponka P. Evaluation of the iron chelation potential of hydrazones of pyridoxal, salicylaldehyde and

2-hydroxy-1-naphthylaldehyde using the hepatocyte in culture. Hepatology 1992;15:492–501.

[23] Johnson DK, Pippard MJ, Murphy TB, Rose NJ. An *in vivo* evaluation of iron-chelating drugs derived from pyridoxal and its analogs. J Pharmacol Exp Ther 1982;221:399–403.

[24] Baker E, Vitolo ML, Webb J. Iron chelation by pyridoxal isonicotinoyl hydrazone and analogues in hepatocytes in culture. Biochem Pharmacol 1985;34:3011–7.

[25] Carter DC, Ho JX. Structure of serum albumin. Adv Protein Chem 1994;45:153–203.